

Optical properties and growth mechanism of multiple type-II ZnTe/ZnSe quantum dots grown by migration-enhanced epitaxy

Y. Gong,¹ W. MacDonald,² G. F. Neumark,¹ M. C. Tamargo,³ and Igor L. Kuskovsky²

¹*Department of Applied Physics and Applied Mathematics, Columbia University, New York, New York 10027, USA*

²*Department of Physics, Queens College of CUNY, Flushing, New York 11367, USA*

³*Department of Chemistry, City College of CUNY, New York, New York 10036, USA*

(Received 10 August 2007; revised manuscript received 21 January 2008; published 9 April 2008)

The properties of multiple type-II ZnTe/ZnSe quantum dots (QDs), which are coexistent with isoelectronic centers formed by Te, grown by migration-enhanced epitaxy, are studied. The samples with a single deposition cycle of Zn-Te-Zn sandwiched between ZnSe barriers are investigated via temperature- and excitation-dependent photoluminescence (PL) as well as magneto-PL measurements. It is found that the PL consists of two broad bands: a “blue” band, which is dominant at low temperatures, and a “green” band, which is observed at $T \geq 60$ K. Upon increasing the excitation intensity by about 4 orders of magnitude, the peak energy position of the blue band remains nearly the same, whereas the green band exhibits a large blueshift of ~ 50 meV, which suggests that the green band is due to, at least partially, the recombination of excitons bound to type-II QDs. The existence of type-II ZnTe/ZnSe QDs is further supported by the results of magneto-PL, for which the oscillation in the PL intensity as a function of magnetic field is observed. The properties of ZnTe/ZnSe QDs grown under the same Zn/Te flux ratio but with one and three contiguous deposition cycles of Zn-Te-Zn are compared. It is concluded that type-II QDs are formed in both types of samples; however, the density, size, and chemical composition of QDs strongly depend on the deposition of the submonolayer quantities of ZnTe.

DOI: [10.1103/PhysRevB.77.155314](https://doi.org/10.1103/PhysRevB.77.155314)

PACS number(s): 78.67.Hc, 78.66.Hf, 81.07.Ta, 61.46.-w

INTRODUCTION

Over the past decades, there have been intensive studies on the properties of quantum dots (QDs) for their device fabrication potential and interesting physical properties. Most of the studies on self-assembled quantum dots are carried out on so-called type-I QDs, whereas fewer reports are found on type-II QDs. Recently, however, there have been increased interest in such systems (see, e.g., Refs. 1–5, and references therein) due to their unique properties. Among many systems, type-II ZnTe/ZnSe QDs appear interesting and useful because of their relatively large valence band [0.8 and 1.0 eV (Refs. 6 and 7)] and conduction band offsets. Moreover, the photoluminescence (PL) of bulk ZnSe_{1-x}Te_x alloys is now well studied, which allows one to separate QD PL from that of impurity centers.⁸ In general, the PL from a dilute ZnSe_{1-x}Te_x ($x \leq 4\%$) alloy is attributed to the recombination of excitons bound to isoelectronic centers (ICs), which are formed by n ($n \geq 2$) Te nearest-neighbor atoms substituting Se.^{9,10} It is thus apparent that the PL of a Zn-Se-Te system will strongly depend on its overall structure and growth conditions.^{8,11} Moreover, it was shown that the formation of QDs is due to the continuous growth of Te_{*n*} ICs (i.e., there is a transition from ICs to QDs).^{8,11}

In this paper, we investigate samples similar to those studied in Ref. 8, but grown with one instead of three contiguous deposition cycles of Zn-Te-Zn sandwiched between ZnSe barriers. We thus show that type-II ZnTe/ZnSe QDs are also formed in the Zn-Se-Te multilayer grown with only one deposition cycle of Zn-Te-Zn. Henceforth, we denote samples grown with one and three consecutive Zn-Te-Zn deposition cycles as δ -ZnSe:Te and δ^3 -ZnSe:Te, respectively. It is found that the PL of the δ -ZnSe:Te sample mostly consists of two main emission bands: one centered at

~ 2.7 eV (“blue” band) and another centered at ~ 2.5 eV (“green” band). At low temperature ($T=10$ K), the PL is dominated by the blue band; with increasing temperature, the relative intensity of the green band increases. Upon increasing the excitation intensity, the green band exhibits a large blueshift, which is the characteristic feature of PL related to quantum structures with type-II band alignment, whereas the blue band shows nearly no changes and is attributed to isoelectronic bound excitons (IBEs).⁸ The existence of type-II QDs in the δ -ZnSe:Te sample is further confirmed by the results of magneto-PL, where oscillation of the integrated PL intensity as a function of the magnetic field is observed. This is consistent with the previous theoretical studies (e.g., Refs. 12 and 13, and reference therein), which predicted that the PL intensity and the exciton energy will oscillate in type-II QDs. Finally, to gain insight on the formation mechanism and optimize the growth conditions for ZnTe/ZnSe QDs, we compared the results of secondary ions mass spectroscopy (SIMS) and high resolution x-ray diffraction (HRXRD) measurements of a pair of samples grown under the same Zn/Te flux ratio but with a single and three contiguous deposition cycles of Zn-Te-Zn. It is found that the δ -ZnSe:Te sample has a much lower Te concentration in the QD-containing regions than that of the δ^3 -ZnSe:Te sample.

EXPERIMENT

The multiple ZnTe/ZnSe QDs were grown on (001) GaAs substrates in a Riber 2300 molecular beam epitaxy (MBE) system. A ZnSe barrier was first grown for t_{ZnSe} seconds, and then the Se shutter was closed for 5 s to interrupt the growth and produce a Zn-terminated surface. After this, all shutters were closed for 5 s to desorb the excess Zn from the surface, and then the Te shutter was opened to deposit Te

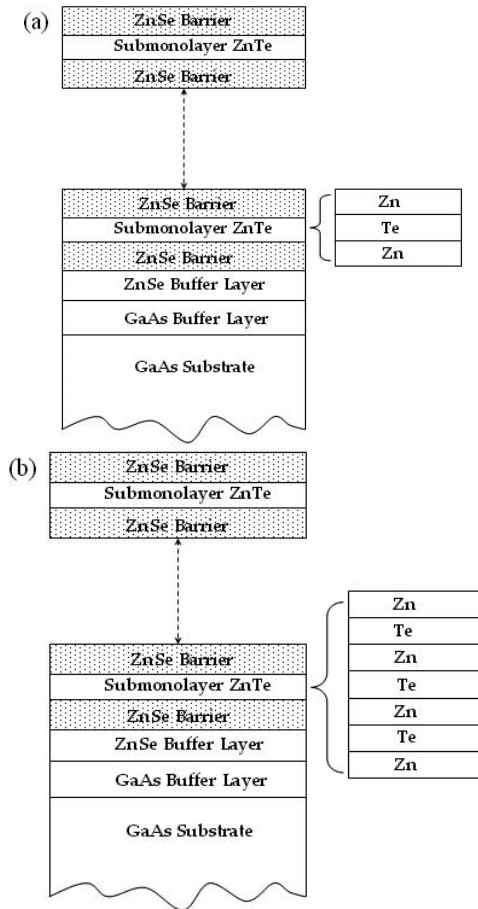


FIG. 1. Growth structure of multiple type-II ZnTe/ZnSe quantum dots with (a) one deposition cycle of Zn-Te-Zn (i.e., δ -ZnSe:Te) and (b) three consecutive deposition cycles of Zn-Te-Zn (i.e., δ^3 -ZnSe:Te).

on the Zn-terminated surface for 5 s. After another growth interruption for 5 s, the Zn shutter was opened for 5 s to evaporate Zn, followed by the growth of the next ZnSe barrier. It is important to note that only submonolayer quantities of ZnTe were deposited between ZnSe barriers. Such a sequential deposition of elements is often referred to as migration-enhanced epitaxy (MEE).¹⁴ MEE is based on chemical reactions at the heated surface of a solid substrate, onto which the constituent elements of the compound to be grown are deposited sequentially as pulses of neutral molecules or atoms. In solid-source MBE, the deposition pulses are generated by the opening and closing of fast shutters. MEE is highly suitable for QD growth since, in this case, controlled surface migration during growth is important.^{14,15} A delay time, during which the deposition process is interrupted, allows for (i) smoothing by enhanced surface migration, (ii) increased surface migration of deposited elements, and (iii) reevaporation of adatoms of the deposited species, which are in excess of the first chemisorbed monolayer. It can be argued that the ability of Te adatoms to migrate “freely” over the surface contributes to the formation of QDs out of Te_n isoelectronic centers as proposed in Refs. 8. This growth sequence was repeated over 100 times and δ -ZnSe:Te samples were obtained. When the deposition of

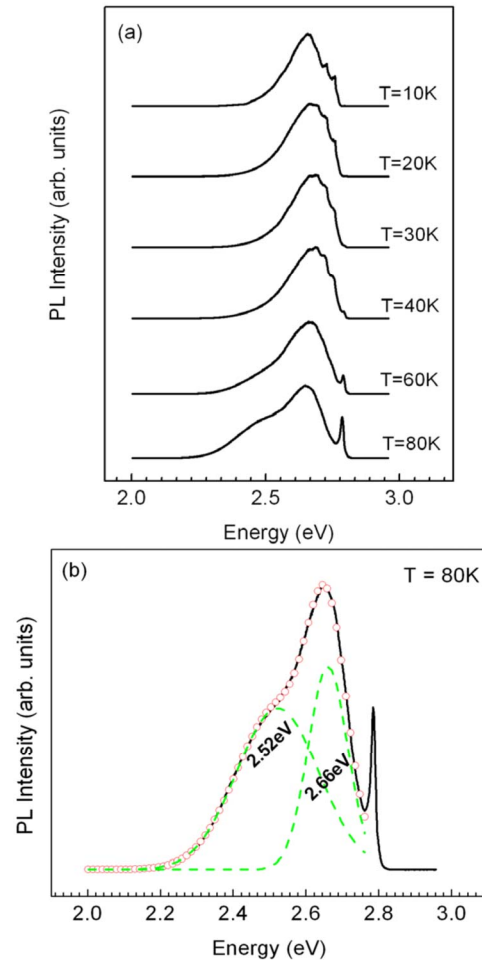


FIG. 2. (Color online) (a) PL spectra from a δ -ZnSe:Te sample measured at various temperatures. (b) Two Gaussian fits of the PL at 80 K. The peaks are centered at ~ 2.52 eV (green band) and ~ 2.66 eV (blue band). The solid line represents the experimental result; red open circles and green dashed lines are from the fitting.

Zn-Te-Zn was repeated for three consecutive times, δ^3 -ZnSe:Te samples were obtained. Figs. 1(a) and 1(b) show the basic structures of both types, respectively.

The low-temperature and temperature-dependent PL measurements were carried out by using a closed cycle refrigerating system. The 325 nm emission line from a He-Cd laser was used as the excitation source, and the excitation intensity can be varied by over 4 orders of magnitude with the aid of the neutral density filters mounted on a dual-wheel holder in front of the laser. The emitted light was dispersed through a $\frac{3}{4}$ m monochromator and was then detected with a thermoelectrically cooled GaAs photomultiplier tube coupled to a photon counter. Magneto-PL measurements were performed at the National High Magnetic Field Laboratory. The magneto-PL was recorded at 4.2 K in the Faraday configuration with a magnetic field of up to 31 T.

HRXRD measurements were carried out at Beamline X20A at the National Synchrotron Light Source (NSLS), Brookhaven National Laboratory (BNL). All measurements were made using the monochromatic synchrotron radiation at 8 keV with a double-crystal Ge (111) monochromator. To

enhance the angular resolution, a Ge (111) analyzer was placed in front of the detector.

RESULTS AND DISCUSSION

Fig. 2(a) shows the temperature-dependent PL spectra from a δ -ZnSe:Te sample under the maximum excitation intensity (I_{\max}) of our experimental conditions. At low temperatures, $T \leq 40$ K, the PL spectra are dominated by a single broad band centered at around 2.70 eV with sharp lines on the higher energy side. We note that these sharp lines are clearly observed only in some δ -ZnSe:Te samples with nominally very low Te fraction; samples that have relatively high Te fraction show shoulders instead of clear PL lines. These sharp lines are tentatively attributed to excitons bound to pairs of Te atoms.^{16,17} However, more detailed studies are required to draw a final conclusion about the microscopic nature of the centers (see also discussion in Ref. 18). As we are interested in the emission related to quantum dots, we will focus on the broad bands.

When the temperature is increased above 60 K, another broad peak appears as a lower energy shoulder of the dominant peak, becoming more pronounced with a further increase in the temperature. As an example, in Fig. 2(b), we show the PL spectrum measured at $T=80$ K, which was fitted by two Gaussian peaks: a "blue band" centered at 2.66 eV and a "green band" centered at 2.52 eV.

To further study the origin of the observed green and blue emissions, intensity-dependent PL was measured on this δ -ZnSe:Te sample at $T=80$ K since at the lower temperatures, the green band does not have sufficient intensity, whereas above 80 K, the overall intensity of the emission is too low to perform meaningful power studies in a wide range of excitation intensities. The recorded PL spectra were fitted by two Gaussian peaks, and the peak energy positions of both green and blue bands as a function of the excitation

intensity are plotted in Fig. 3. It is found that the peak energy of the green band exhibits a large (~ 50 meV) shift to higher energies upon increasing the excitation intensity by about 4 orders of magnitude, whereas the blue band barely shows any spectral shift. This suggests different origins of the green and blue bands.

First, we discuss the origin of the green band. The blue-shift of emission spectra with increasing excitation intensity has been previously reported for various type-II quantum structures and a band bending model at the interface has been proposed to explain this behavior.¹⁹⁻²¹ For our material structure, due to the large valence band offset between ZnTe and ZnSe, the holes are strongly confined in ZnTe QDs, while electrons are localized in ZnSe barriers. Due to Coulomb interaction, an electric field across the interface is formed, resulting in band bending near the ZnTe/ZnSe interface. With an increase in the excitation intensity, more electron and hole pairs are excited and the band bending effect becomes more pronounced. It is expected that the emission spectra will shift toward higher energies with increasing excitation intensity. Thus, the green band is due to, at least partially, the recombination of excitons within type-II quantum structures¹⁹⁻²² and QDs in particular (see below). Moreover, as shown in Fig. 3 (the red dashed line), here the peak energy shift follows the cube root of the excitation intensity.^{8,23}

The blue emission exhibits very little shift (~ 6 meV) when the excitation intensity is increased by about 4 orders of magnitude. A plausible origin of the blue band is the recombination of excitons bound to ICs formed by Te_n centers (the small shift observed here is probably due to an overlap with the green band). The PL due to IBEs has been widely reported for dilute bulk $\text{ZnSe}_{1-x}\text{Te}_x$ ($x \leq 4\%$) alloys as well as for ZnTe/ZnSe quantum wells.²⁴ Moreover, in our previous work on the δ^3 -ZnSe:Te samples,⁸ a blue band, which does not shift with increasing excitation intensity, was also

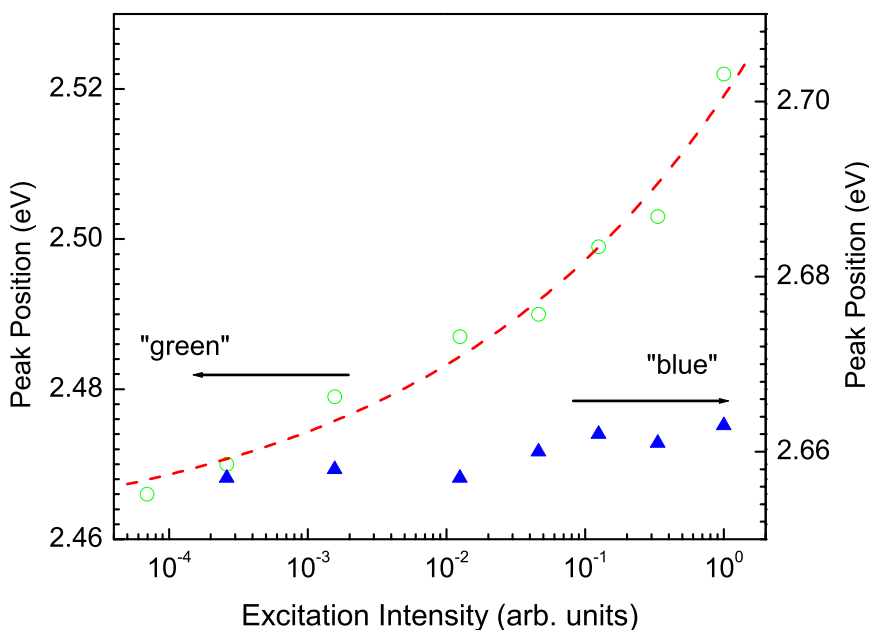


FIG. 3. (Color online) The PL peak positions of both green and blue bands as a function of the excitation intensity. The red dashed line is the fitting of the peak energy as the cube root of the excitation intensity.

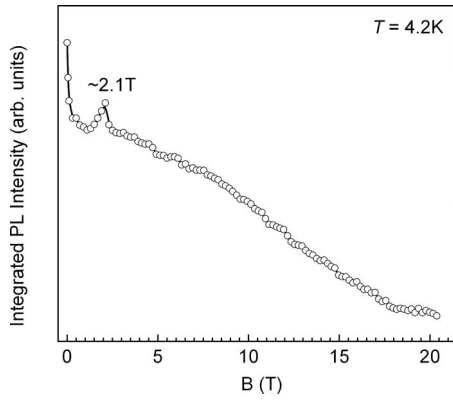


FIG. 4. Integrated PL intensity of a δ -ZnSe:Te sample as a function of magnetic field B .

reported. Furthermore, detailed studies^{8,18} of temperature-dependent PL, PL excitation, and time-resolved PL show that the blue band is, indeed, due to IBEs. Thus, the δ -ZnSe:Te samples also contain both type-II quantum structures and isoelectronic centers.

To support such a conclusion, we point out that the PL at various excitation intensities was also measured at 10 K, but no peak energy shift was observed. Assuming that there is a low density of ZnTe/ZnSe QDs formed in the δ -ZnSe:Te sample, which is plausible due to the low concentration of Te (see below), the emission due to IBE will dominate at lower temperatures. With increasing temperature, the excitons bound to ICs ionize. Although the weakly bound electrons of type-II excitons can also ionize, the holes are still strongly confined in the QDs, so the electrons are eventually recaptured and radiatively recombine with the holes.⁸ Accordingly, the PL will be dominated by the QD-related emission up to relatively high temperatures. We note that the PL of the δ^3 -ZnSe:Te sample is dominated by the QD-related emission even at 10 K, which indicates the formation of a high density of ZnTe/ZnSe QDs.

The existence of type-II QDs (rather than type-II quantum wells) is further supported by the results of magneto-PL. Fig. 4 plots the integrated PL intensity of a δ -ZnSe:Te sample as a function of the magnetic field B along the growth direction. The major feature here is the presence of a peak in the integrated intensity at $B_0 \approx 2.1$ T. The overall decrease in the intensity is attributed to magnetic-field-induced carrier localization.² The observed dependence of the PL intensity on the magnetic field is consistent with the predicted optical Aharonov–Bohm effect for type-II QDs of cylindrical symmetry (see, e.g., Refs. 12 and 25) and is similar to the observations for the δ^3 -ZnSe:Te samples.² A detailed discussion and additional references for the PL intensity as a function of the magnetic field for the Zn-Se-Te multilayers can be found in Ref. 2. Qualitatively, the observed behavior of the PL intensity can be understood following the arguments of Ref. 25. Assuming a cylindrical symmetry for the QDs, the δ -ZnSe:Te sample can be considered as stacks of multiple ZnTe disks buried in ZnSe barriers; holes are confined within the disks, while electrons are localized in the ZnSe barriers. With increasing magnetic field, the electron (in the ground

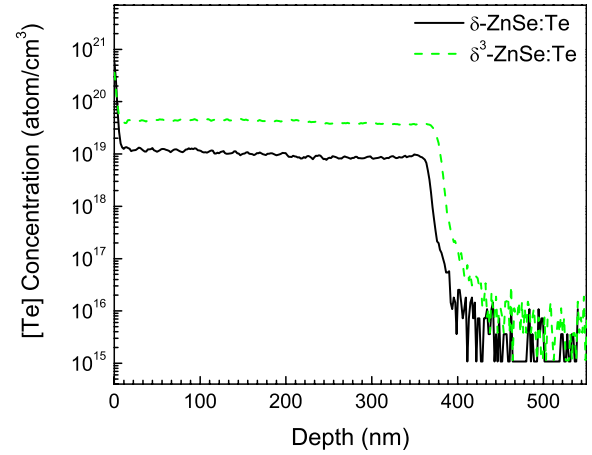


FIG. 5. (Color online) SIMS profiles of the δ -ZnSe:Te sample (black solid line) and the δ^3 -ZnSe:Te sample (green solid line).

state, $l_e=0$) gets closer to the QDs, which increases its energy due to the barrier created by the QDs. When the magnetic field reaches certain value, B_0 , it is more favorable for the electron to “jump” to the next orbit with the nonzero orbital momentum ($l_e=-1$), which is farther from the dot. However, the selection rule requires that the total orbital momentum of the exciton ($L=l_e+l_h$) is equal to zero (e.g., Refs.

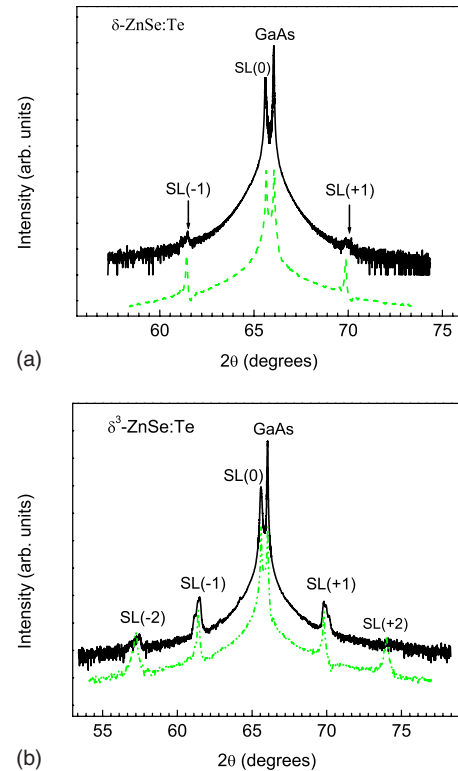


FIG. 6. (Color online) HRXRD of Zn-Se-Te multilayers with submonolayer insertions of ZnTe. Solid lines represent (004) ω - 2θ scans of (a) a δ -ZnSe:Te sample and (b) a δ^3 -ZnSe:Te sample. The green dashed lines are results of simulation based on dynamical diffraction theory. All curves are plotted with intensity in the logarithmic scale, and the results of experiment and simulation are shifted vertically for clarity.

TABLE I. Structural parameters obtained by simulating high resolution x-ray diffraction curves based on dynamical diffraction theory.

Sample	[Te] in the barriers	[Te] in the QD-containing layers	Thickness of the barriers (Å)	Average thickness of QD-containing layers (Å)	$\sigma(T)$ (Å)
δ -ZnSe:Te	~ 0.015	~ 0.30	~ 24.0	~ 0.7	~ 0.7
δ^3 -ZnSe:Te	~ 0.02	~ 0.50	~ 24.0	~ 0.7	~ 0.7

12 and 25) and, thus, the radiative transition becomes forbidden (dark exciton state). As a result, the PL intensity will decrease. The sharp peak arises due to the increase in the PL intensity with higher magnetic field for $B \leq B_0$ because of the increased overlap of the electron and hole wave functions. The value of the magnetic field B_0 allows one to estimate the lateral size of the dots: the higher the field, the smaller the dots. The highest value for B_0 reported in Ref. 2 was 1.79 T, which suggests that the QDs formed in the δ -ZnSe:Te sample are, indeed, smaller. By assuming that the model developed in Ref. 25 is valid for our multilayered systems, we estimate the radius of the quantum dots to be about 9 nm.

Finally, we investigated the dependence of the growth condition on the properties of our samples. Here, we compared a pair of samples grown under the same Zn/Te flux ratio but with one and three consecutive deposition cycles of Zn-Te-Zn sandwiched between ZnSe barriers. Fig. 5 shows the SIMS profile of both samples. Although both samples were grown with the same Zn/Te flux ratio, the average [Te] concentration in the δ^3 -ZnSe:Te sample is about three times higher than that in the δ -ZnSe:Te sample.²⁶ The higher average [Te] concentration in the δ^3 -ZnSe:Te sample is likely due to the higher [Te] concentration in the QD-containing regions. We further show in Fig. 6 the symmetric (004) ω - 2θ scans of these samples. For both samples, the sharp peak with the highest intensity is the (004) reflection of the GaAs substrate and the zero-order satellite [SL(0)] peak is located at the small-angle side of the GaAs peak, due to the larger lattice parameters of ZnSe and ZnTe than that of GaAs. On both sides of the SL(0) peak, higher order satellite peaks, distributed with nearly equal angular distances, are observed due to the long-range periodicity along the growth direction, formed by depositing submonolayer quantities of ZnTe between ZnSe barriers. SL peaks up to the second order are observed for the δ^3 -ZnSe:Te sample, whereas only very weak first-order SL peaks are observed for the δ -ZnSe:Te sample. This implies that there is a lower Te concentration in the QD-containing regions for the δ -ZnSe:Te sample. We note that compared with the SL(0), higher order satellites are broadened, which indicates that there are fluctuations in the thickness of different periods [represented by period dispersion, $\sigma(T)$].

The structural parameters including the average thickness of the QD-containing region and the barriers as well as the corresponding [Te] concentrations were determined by simu-

lating the measured HRXRD curves based on dynamical diffraction theory^{27,28} (for a detailed description of the simulation procedure, see Ref. 29). The simulated diffraction curves are plotted in Fig. 6 as green dashed lines and the extracted structural parameters are listed in Table I. Based on the simulation results, it is found that the δ -ZnSe:Te and δ^3 -ZnSe:Te samples have the same period and nearly the same [Te] concentrations in the barriers ($x \leq 0.02$). However, the average [Te] concentration in the QD-containing regions is much higher for the latter, which is in agreement with the SIMS data.

CONCLUSIONS

We studied the properties of multiple type-II ZnTe/ZnSe quantum dots formed by a single deposition cycle of Zn-Te-Zn (δ -ZnSe:Te) sandwiched between ZnSe barriers. Temperature- and excitation-dependent PL as well as magneto-PL measurements confirmed the formation of ZnTe/ZnSe quantum dots. Compared to a typical sample grown with three consecutive deposition Zn-Te-Zn cycles (δ^3 -ZnSe:Te sample), the low-temperature PL of a δ -ZnSe:Te sample is dominated by the recombination of excitons bound to isoelectronic Te centers, which is due to the low density of ZnTe/ZnSe quantum dots. The average size of QDs (~ 9 nm) is smaller than that of the QDs formed in typical δ^3 -ZnSe:Te samples. Finally, SIMS and HRXRD measurements of a pair of δ -ZnSe:Te and δ^3 -ZnSe:Te samples, grown under the same Zn/Te flux ratio, showed that the chemical compositions of QDs depend on the deposition cycles of the submonolayer quantities of ZnTe. Therefore, the size, density, and chemical composition of the quantum dots can be controlled by varying the parameters of Te deposition.

ACKNOWLEDGMENTS

We would like to acknowledge support from DOE Grant No. DE-FG02-05ER46219. One of us (I.L.K.) also recognizes support from PSC-CUNY Grant No. 69700-0038. Part of this work was performed at the NSLS, BNL, which is supported by DOE under Contract No. DE-AC02-98CH10886, and at the NHMFL, which is supported by NSF (Cooperation Agreement No. DMR-0084173) and by the State of Florida.

- ¹C. Y. Jin, H. Y. Liu, S. Y. Zhang, Q. Jiang, S. L. Liew, M. Hopkinson, T. J. Badcock, E. Nabavi, and D. J. Mowbray, *Appl. Phys. Lett.* **91**, 021102 (2007).
- ²I. L. Kuskovsky, W. MacDonald, A. O. Govorov, L. Mourokh, X. Wei, M. C. Tamargo, M. Tadic, and F. M. Peeters, *Phys. Rev. B* **76**, 035342 (2007).
- ³J. R. Madureira, M. P. F. de Godoy, M. J. S. P. Brasil, and F. Iikawa, *Appl. Phys. Lett.* **90**, 212105 (2007).
- ⁴N. Suzuki, T. Anan, H. Hatakeyama, and M. Tsuji, *Appl. Phys. Lett.* **88**, 231103 (2006).
- ⁵A. A. Toropov, I. V. Sedova, O. G. Lyublinskaya, S. V. Sorokin, A. A. Sitnikova, S. V. Ivanov, J. P. Bergman, B. Monemar, F. Donatini, Le Si Dang, *Appl. Phys. Lett.* **89**, 123110 (2006).
- ⁶F. Malonga, D. Bertho, C. Jouanin, and J. M. Jancu, *Phys. Rev. B* **52**, 5124 (1995).
- ⁷S.-H. Wei and A. Zunger, *Phys. Rev. B* **53**, R10457 (1996).
- ⁸Y. Gu, I. L. Kuskovsky, M. van der Voort, G. F. Neumark, X. Zhou, and M. C. Tamargo, *Phys. Rev. B* **71**, 045340 (2005).
- ⁹I. V. Akimova, A. M. Akhekyan, V. I. Kozlovsky, Y. V. Korostelin, and P. V. Shapin, *Sov. Phys. Solid State* **27**, 1041 (1985).
- ¹⁰S. Permogorov and A. Reznitsky, *J. Lumin.* **52**, 201 (1992).
- ¹¹M. Jo, M. Endo, H. Kumano, and I. Suemune, *J. Cryst. Growth* **301-302**, 277 (2007).
- ¹²A. O. Govorov, S. E. Ulloa, K. Karrai, and R. J. Warburton, *Phys. Rev. B* **66**, 081309(R) (2002).
- ¹³M. Grochol, F. Grosse, and R. Zimmermann, *Phys. Rev. B* **74**, 115416 (2006).
- ¹⁴Y. Horikoshi, *Semicond. Sci. Technol.* **8**, 1032 (1993).
- ¹⁵K. Leonardi, H. Heinke, K. Ohkawa, D. Hommel, H. Selke, F. Gindele, and U. Woggon, *Appl. Phys. Lett.* **71**, 1510 (1997).
- ¹⁶I. L. Kuskovsky, C. Tian, G. F. Neumark, J. E. Spanier, I. P. Herman, W. C. Lin, S. P. Guo, and M. C. Tamargo, *Phys. Rev. B* **63**, 155205 (2001).
- ¹⁷A. Muller, P. Bianucci, C. Piermarocchi, M. Fornari, I. C. Robin, R. Andre, and C. K. Shih, *Phys. Rev. B* **73**, 081306(R) (2006).
- ¹⁸Y. Gu, I. L. Kuskovsky, and G. F. Neumark, in *Wide Bandgap Light Emitting Materials and Device*, edited by G. F. Neumark, I. L. Kuskovsky, and H. X. Jiang (Wiley-VCH, New York, 2007), p. 216.
- ¹⁹Y. S. Chiu, M. H. Ya, W. S. Su, and Y. F. Chen, *J. Appl. Phys.* **92**, 5810 (2002).
- ²⁰E. R. Glaser, B. R. Bennett, B. V. Shanabrook, and R. Magno, *Appl. Phys. Lett.* **68**, 3614 (1996).
- ²¹F. Hatami, M. Grundmann, N. N. Ledentsov, F. Heinrichsdorff, R. Heitz, J. Bohrer, D. Bimberg, S. S. Ruvimov, P. Werner, V. M. Ustinov, P. S. Kopev, and Zh. I. Alferov, *Phys. Rev. B* **57**, 4635 (1998).
- ²²K. Leonardi, H. Heinke, K. Ohkawa, D. Hommel, H. Selke, F. Gindele, U. Woggon, *Phys. Rev. B* **52**, 14058 (1995).
- ²³T. T. Chen, C. L. Cheng, Y. F. Chen, F. Y. Chang, H. H. Lin, C. T. Wu, and C. H. Chen, *Phys. Rev. B* **75**, 033310 (2007).
- ²⁴K. Suzuki, U. Neukirch, J. Gutowski, N. Takojima, T. Sawada, and K. Imai, *J. Cryst. Growth* **184/185**, 882 (1998).
- ²⁵K. L. Janssens, B. Partoens, and F. M. Peeters, *Phys. Rev. B* **64**, 155324 (2001).
- ²⁶We note that since the barriers are extremely thin, it is very hard to resolve the periodic variation of [Te] along the growth condition. See also I. L. Kuskovsky, Y. Gu, Y. Gong, H. F. Yan, J. Lau, I. C. Noyan, G. F. Neumark, O. Maksimov, X. Zhou, M. C. Tamargo, V. Volkov, Y. Zhu, and L. Wang, *Phys. Rev. B* **73**, 195306 (2006).
- ²⁷S. Takagi, *Acta Crystallogr.* **15**, 1311 (1962).
- ²⁸D. Taupin, *Bull. Soc. Fr. Mineral. Cristallogr.* **88**, 469 (1964).
- ²⁹Y. Gong, H. F. Yan, I. L. Kuskovsky, Y. Gu, I. C. Noyan, G. F. Neumark, and M. C. Tamargo, *J. Appl. Phys.* **99**, 064913 (2006).